A Wireless Batch Sealed Absolute Capacitive Pressure Sensor

Orhan Akar[1], Tayfun Akin[1], Tim Harpster[2], and Khalil Najafi[2]
[1]Middle East Technical University, Dept. of Electrical and Electronics Eng., Ankara, Turkey
[2]Center for Integrated Microsystems, The University of Michigan, Ann Arbor, MI 48109
e-mail: tayfun-akin@metu.edu.tr http://www.eee.metu.edu.tr/~tayfuna

Summary. *This paper reports the development of an absolute wireless capacitive pressure sensor. The sensor has a simple structure and is obtained using a capacitive pressure sensor and a gold-electroplated planar coil that form an LC circuit. Applied pressure deflects the 6 μm-thin silicon diaphragm, changing the capacitance, and hence, the resonant frequency of the circuit. This change is sensed remotely with inductive coupling, eliminating the need for wire connection or implanted RF telemetry circuits to monitor the applied pressure. The sensor is fabricated using boron-etch stop technique. Fabricated devices measure 2.6x1.6 mm² in size and houses 24 turns of gold-electroplated coil that has a measured inductance of 1.2 μH. The sensor is designed to provide a resonant frequency change between 95-103MHz for a pressure change in the range 0-50mmHg w.r.t. the ambient pressure, providing a pressure responsivity and sensitivity of 160 KHz/mmHg and 1553ppm/mmHg, respectively. The measured pressure responsivity and sensitivity of the fabricated device are 120KHz/mmHg and 1579ppm/mmHg, respectively.*

Keywords: wireless sensor, sealed sensor, and capacitive pressure sensor

Introduction

Absolute pressure sensors are required in many applications, including industrial process control, environmental monitoring, and biomedical systems. Capacitive pressure sensors provide very high pressure sensitivity, low noise, and low temperature sensitivity and are preferred in many emerging high-performance applications. However, to fabricate absolute pressure sensors with sealed cavities that also allow easy lead transfer from inside of the cavity to outside requires relatively complex fabrication technologies [1]. In addition to the need for batch-sealed absolute pressure sensors, many emerging applications require these sensors to operate via a wireless link. One such application is in continuous long-term monitoring of the pressure for various medical applications [2]. Some wireless telemetry systems use active transmitters, however, these devices are often big and require a power source in the form of an implanted battery, or an implanted active circuit that can receive power through inductive telemetry [3]. Both of these complicate the system design and operation.

This paper presents a new structure for wireless absolute capacitive pressure sensors. The structure utilizes a parallel inductor-capacitor resonant circuit. The capacitor is formed by the pressure sensor and changes in response to changes in pressure. The on-chip inductor is fabricated inside the sealed cavity of the sensor and is connected to the pressure sensitive capacitor. Because the inductor is inside the sealed cavity of the pressure sensor, lead transfer outside of the cavity is not needed, which in turn allows one to batch seal pressure sensors at the wafer level. Furthermore, the sensor can be operated using a passive telemetry approach [4-7], as discussed later.

Sensor structure

Figure 1 shows the structure of the wireless pressure sensor. It consists of a boron-doped silicon diaphragm with a thickness of ~3-6μm, which is supported by anchors that fix it to a glass substrate. The diaphragm is suspended over the glass by a gap of about 2μm and can deflect when the pressure across it changes. This forms a variable-gap capacitor. To obtain high pressure sensitivity, the capacitive gap should be as small as possible, usually in the range of 1-2μm. The capacitor gap should also house the gold-electroplated coil. The planar coil is placed in a recessed glass area around the metal capacitor plate on the glass. By making the recess as deep as possible, it is possible to fabricate very thick on-chip coils with high Q. This is necessary to obtain high sensitivity for the sensor. Figure 2 shows the cross-section and electrical equivalent of the wireless pressure sensor. The variable capacitor and the electroplated coil inside it form an LC circuit, whose resonant frequency changes with the applied pressure. The change in the resonant frequency is sensed remotely with inductive coupling, eliminating the need for wire connection to monitor the applied pressure.

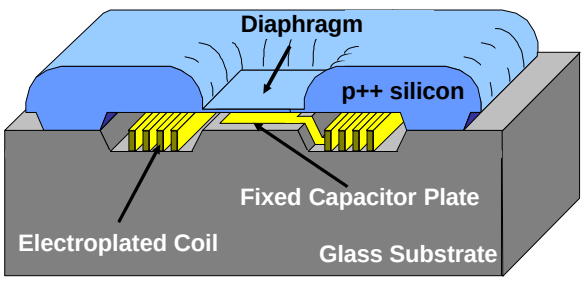

Fig. 1: Structure of the wireless pressure sensor.

ISBN 87-89935-50-0

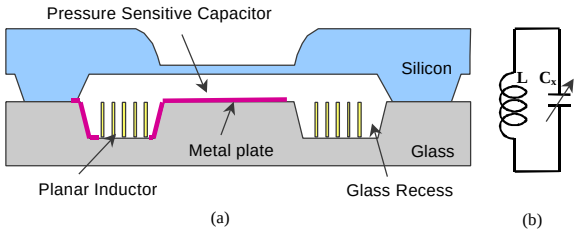

Fig. 2: Wireless capacitive pressure sensor: (a) cross-section, (b) electrical equivalent. The change in the resonance frequency due to capacitance change is sensed remotely with inductive coupling, eliminating the need for wire connection.

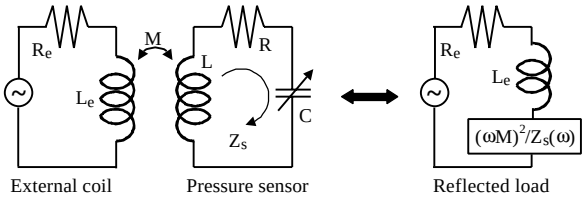

Fig. 3: Equivalent circuit model of the telemetric readout approach.

Inductive coupling link

Figure 3 shows the equivalent circuit model of the inductive coupling link used in the telemetric readout. The sensor is modeled with an inductor, L, a series resistance of the inductor, R, and a variable capacitor, C. The resonance frequency of the sensor is given by

$$f_0 = \frac{1}{2\pi\sqrt{LC}} \qquad \text{(Eq.1)}$$

The resonance frequency changes in response to pressure and it can be detected by inductive telemetry with an external coil antenna. Due to inductive coupling, the external coil stimulates the sensor circuit, and the load impedance is reflected back to the antenna. Reflected impedance, X_l, can be found as a function of the sensor impedance, Z_s, and the mutual inductance, M, between the coil antenna and the integrated inductance in the sensor, as

$$X_l = \frac{(\omega M)^2}{Z_s(\omega)} \qquad \text{(Eq.2)}$$

where,

$$M = k\sqrt{L_e L} \qquad \text{(Eq.3)}$$

$$Z_s(\omega) = R + j\left(\omega L - \frac{1}{\omega C}\right) \qquad \text{(Eq.4)}$$

where ω is the angular frequency, k is the coupling coefficient. The impedance seen at the external coil due to coupling is given by [8-9]

$$Z(\omega) = R_e + j\omega L_e + \frac{(\omega M)^2}{Z_s(\omega)} \qquad \text{(Eq.5)}$$

where R_e and L_e are the series resistance and the inductance of the external coil. At the resonant frequency of the pressure sensor equivalent circuit, the impedance Z_s becomes purely resistive and reduces to only R, therefore, the impedance of the external antenna becomes

$$Z(\omega_o) = R_e + j\omega_o L_e + \frac{(\omega_o M)^2}{R} \qquad \text{(Eq.6)}$$

By monitoring overall impedance change of the external coil due to the reflected impedance, it is possible to detect the sensor resonance frequency. This change is more detectable if the phase of the Z is monitored. The approximate magnitude of the impedance phase dip is given by

$$\Delta\varphi_{DIP} \cong \tan^{-1}\left(\frac{\omega_o M^2}{L_e R}\right) \qquad \text{(Eq.7)}$$

The impedance phase dip is maximized when the series resistance of the electroplated coil, i.e., R, is minimized and its inductance, L, is maximized for larger M. However, it is important to note that, when L is increased by increasing the number of turns in the coil, then the parasitic capacitance of the coil also increases, decreasing the self resonant frequency of the planar coil [8-9]; but, the coil self resonant frequency should be much higher then the operating frequency for proper device operation. Therefore, it is more important to decrease the series resistance of the electroplated coil for a sensitive detection of the resonant frequency of the sensor. The increase in the series resistance of the coil at high operation frequencies due to skin effects should also be considered during the design phase [9].

Fabrication Process

The fabrication process of the sensor is based on the bulk silicon dissolved wafer process [10] with some additional steps needed to integrate the on-chip electroplated coil with the pressure sensor. A silicon wafer is selectively etched with KOH to create a 2μm recess to define the capacitive gap. Then, two high-temperature boron diffusion steps are applied to define the 12μm support anchors and the 3-6μm diaphragm of the pressure sensor. The diaphragm thickness can be reduced down to 2.5μm if necessary. Meanwhile, a glass wafer is processed to define the fixed plate of the capacitor, which is formed by depositing and patterning a layer of Ti/Pt/Au. The glass wafer is selectively etched to have a 7μm recess, so that 6μm-thick electroplated coil does not touch to the diaphragm of the capacitive pressure sensor when front sides of glass and silicon wafers face each other and are attached using silicon-to-glass anodic bonding.

This process has a number of advantages. It is a simple, batch, and high yield process, and it eliminates the problems associated with the discrete coil attachment. The coil is sealed inside the pressure sensor cavity, so that the harsh external environment does not affect it. It should be noted that for biomedical applications, all the materials used in this process are biocompatible, there is no need for additional protective coatings.

Fabrication and test results

A number of different sensor structures have been designed and fabricated. Figure 4 shows a SEM photograph of the gold electroplated coil windings on the glass substrate. The width and the height of the gold lines are 7μm and 6μm, respectively, while the separation of the lines is 7μm. Figure 5 shows a fabricated sensor seen through the glass substrate. This device measures 2.6mmx1.6mm and houses 24 turns of gold-electroplated coil. Table 1 shows performance parameters of the sensor. The sensor is optimized for a pressure range of 0-50mmHg. Figure 6 shows the SEM photograph of the fabricated sensor showing the cross-sectional view of the capacitive gap. Figure 7 shows another SEM photograph of the fabricated sensor, which is broken to show the electroplated coil windings inside the sealed cavity. Gold electroplated coils are measured to be 1.2μH. With the expected capacitance variation due to changes in pressure, the resonant frequency of the sensor is expected to change between 103 and 95 MHz for a pressure range of 0-50mmHg w.r.t. the ambient pressure, providing a pressure sensitivity of 1553ppm/mmHg and a pressure responsivity of 160KHz/mmHg.

Table 1: Summary of the device characteristics.

Parameter	Value
Diaphragm thickness	6μm
Capacitor plate separation	2μm
Full scale deflection	0.4μm
Dynamic range	0-50mmHg
Total diaphragm area	2x(680x680μm^2)
Device size	2.6mmx1.6mm
Inductance	1.2μH
Capacitance change for 0-50mmHg	2.0-2.35pF
Frequency shift for 0-50mmHg	103-95MHz
Pressure sensitivity	1553ppm/mmHg
Pressure responsivity	160KHz/mmHg

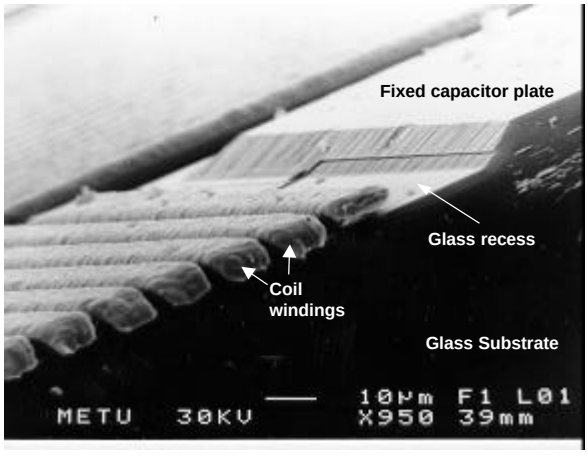

Fig. 4: SEM photograph of the gold electroplated coil windings.

Fig. 5: Photograph of a fabricated sensor seen through the glass substrate. This device measures 2.6mmx1.6mm and houses 24 turns of gold-electroplated coil. The capacitive plate separated into two parts to increase the dynamic range.

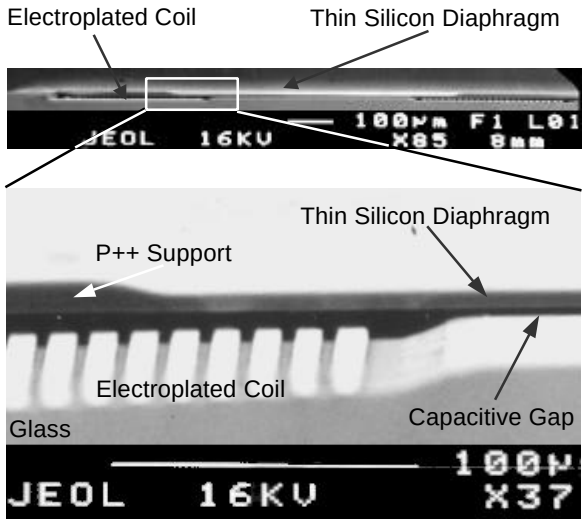

Fig. 6: SEM photograph of a fabricated sensor showing the cross-sectional view.

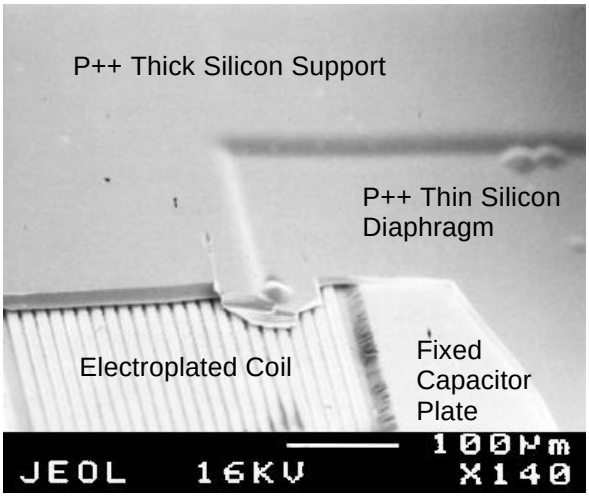

Fig. 7: Another SEM photograph of the fabricated sensor, which is broken to show the electroplated coil windings inside the sealed cavity.

ISBN 87-89935-50-0

A number of measurements were performed to verify the device operation and to characterize its performance. The measurements were completed using an external coil, a pressure chamber, and an impedance analyzer. The phase shift on the external coil due to inductive coupling is monitored using HP 4395A Network/Impedance Analyzer. Figure 8 shows the impedance phase changes on the external stimulating coil at different pressure values w.r.t. the ambient pressure. The monitored resonant frequency chance is between 76MHz and 70MHz in the 0-50mmHg pressure range, resulting in a pressure responsivity of 120kHz/mmHg and a pressure sensitivity of 1580ppm/mmHg. Figure 9 shows remotely detected sensor resonance frequency change with respect to the applied pressure change from zero pressure to the over pressure value of 100mmHg.

It should be noted here that the resonant frequency of the sensor seems lower than the design value. The reason is believed to be the difference between the actual pressure inside the cavity and the ambient pressure. The pressure in the cavity is not ambient pressure, but the applied pressure is monitored with respect to the ambient pressure. The pressure inside the cavity is lower than the ambient pressure, since during the sealing process with electrostatic glass to silicon anodic bonding, the structure is heated upto 400°C. When the device cools down, the air inside the sealed cavity contracts and pulls the diaphragm closer to the fixed metal capacitor plate on the glass, increasing the zero pressure capacitance, hence, decreasing the resonant frequency of the sensor. Although the measured resonant frequency is different than the designed resonant frequency, the measured pressure sensitivity of the device is 1580ppm/mmHg, which very close to the design sensitivity of 1550ppm/mmHg. The device sensitivity can be increased by increasing the device dimensions.

These measurements show that the device is functional and allows to measure the pressure of a sealed capacitive pressure sensor remotely, without requiring lead transfer from the sealed cavity.

Conclusions

An absolute wireless capacitive pressure sensor has been designed and fabricated. The sensor consists of a pressure sensitive capacitor and an integrated inductor forming a pressure sensitive resonant circuit. The resonance frequency of the sensor is measured by inductive telemetry. Fabricated devices measure 2.6x1.6 mm^2 in size and are optimized to provide a dynamic range of 0-50mmHg. The fabricated device is operational, and its resonant frequency is monitored to change between 76MHz and 70MHz when a pressure between 0 and 50mmHg is applied with respect to the ambient pressure. This corresponds to a pressure responsivity and sensitivity of 120KHz/mmHg or 1580ppm/mmHg, respectively.

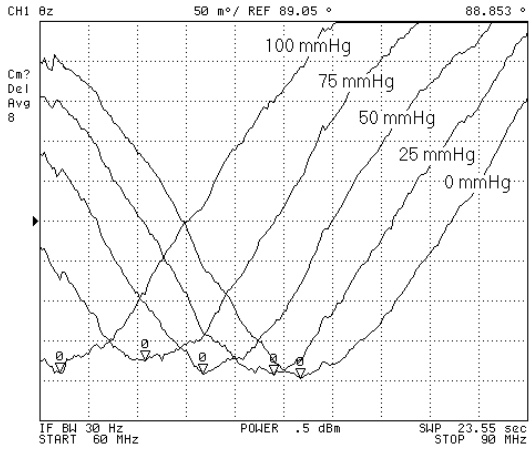

Fig. 8: External coil phase shift due to the resonant frequency shift of the sensor with the applied pressure.

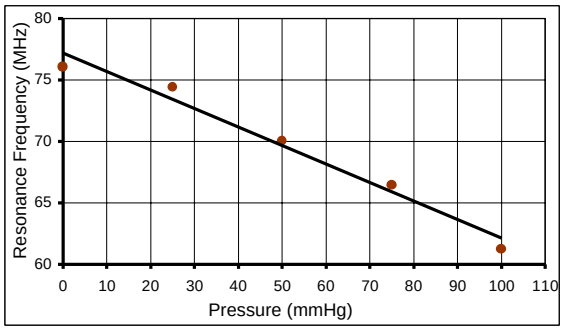

Fig. 9: Resonant frequency change of the sensor with the applied pressure w.r.t. the ambient pressure.

Acknowledgements

This work is supported by NSF-International Grant No: 9602182, which is provided to Prof. Najafi and Prof. Akin for *US-Turkey Cooperative Research.* Authors would like to thank Dr. Babak Ziaie for his valuable discussions.

References

[1] A. Chavan and K. D. Wise. *9th Int. Conf. on Solid-State Sensors & Actuators, (TRANSDUCERS'97)* , June 16-19, Chicago, USA, 1997.

[2] R. Puers. *Sensors&Actuators* A52 (1996), pp. 169-174.

[3] B. Ziaie, M. D. Nardin, A. R. Coghlan, and K. Najafi. *IEEE Trans. on Biomedical Engineering*, Vol. BME-44, No. 10, October 1997

[4] W. N. Carr, S. Chamarti, X. Gu. *8th Int. Conf. on Solid-State Sensors & Actuators (TRANSDUCERS'95) and Eurosensors IX*, pp. 624-627, Stockholm, Sweden, June 25-29, 1995.

[5] J. M. English and M. G. Allen. *IEEE Int. Conf. on Micro Electro Mechanical Systems (MEMS'99)* , pp. 511-516, Orlando, Florida, USA, January 17-21, 1999.

[6] E.C. Park, J.B. Yoon, and E. Yoon. *Jpn. J. Applied Physics*, vol 37 (1998), pp. 7124-7128.

[7] T. Harpster, S. Hauvespre, M. Dokmeci, and K. Najafi. *IEEE Int. Conf. on Micro Electro Mechanical Systems, (MEMS 2000)*, Miyazaki, Japan, Jan. 22-27, 2000.

[8] F. E. Terman. Radio Engineer's Handbook, McGraw-Hill, New York, 1943.

[9] E. G. Weber. Inductance; magnetic materials. Radio Eng. Handbook, K. Henney Ed., McGraw-Hill, 1959.

[10] H. L. Chau and K. D. Wise. IEEE Trans. On Electron Dev., 35-12 (1988) 2355-2362.